

Frequency Diversity Effects of Evaporation Duct Propagation

HERBERT V. HITNEY AND LINDA R. HITNEY

Abstract—A comparison of 3, 9.6, and 18 GHz low-altitude over-the-horizon propagation, as influenced by the evaporation duct, is presented. Both theoretical and experimental results are given for a 35 km over-water path, where the transmitters were located about 5 m above mean sea level and the receivers were located either 4–5 m or 18–19 m above sea level. Results are presented in terms of the one-way propagation factor in decibels at each frequency. Long-term cumulative frequency distributions of calculated and observed propagation factors are presented. Particular attention is given to the relative performance of each radio frequency to investigate frequency-diversity improvements that may be available on such paths. In most cases presented, there is a close agreement of the theory and observations. It is concluded that substantial improvements in received signal levels are likely to be achieved in most areas of the world by a suitable choice of two frequencies in the 10–20 GHz range.

I. INTRODUCTION

THE EVAPORATION duct has been well recognized for many years as a propagation mechanism that can result in substantially higher signals on over-the-horizon, over-water paths at frequencies generally above 3 GHz [1]–[4]. A recent paper by Hitney and Vieth [5] has shown that modern numerical modeling techniques are capable of predicting the statistical propagation effects on such paths with quite good accuracy. Results from their models were compared to measured distributions of signal strength, converted to one-way path loss, for experiments in the Mediterranean and North Sea areas. Both theoretical and experimental results showed median net gains in signal level compared to diffraction theory of 20–30 dB or more for frequencies at 7–18 GHz. All of those results, however, considered only one frequency at a time distributed over periods from a few months to a year. Theoretical considerations suggest that substantial additional improvements to signal level may be achieved using a suitable frequency-diversity scheme. It is our intent in this paper to investigate such additional improvements.

To fairly compare performance of two or more frequencies, one needs to use a signal-level parameter that is independent of frequency. We have chosen to use the one-way propagation factor in this paper, which is defined as the ratio in decibels of the actual signal level to that which would have existed at the same range in free space [6]. Theoretical results that follow are based on omnidirectional antenna patterns, but the measurements were all performed with horizontally pointed directional antennas. To be technically

correct when discussing the experimental results, one should use the term pattern-propagation factor as defined by Kerr [7]. However, for the over-horizon results presented here, there is an insignificant difference between the two factors, and only the first will be used.

Air in immediate contact with the sea surface is nearly saturated with water vapor, and the relative humidity is thus nearly 100%. A few meters above the surface, the relative humidity usually has decreased significantly to a value that depends on many meteorological processes. The rapid decrease of moisture in the first few meters above the surface causes the radio refractive index to decrease much more rapidly than it would in a well-mixed or standard atmosphere. The refractive-index gradient at the lowest heights is such that radio waves refract downwards at a rate exceeding the earth's curvature. As height increases, this gradient and the radio wave's curvature decrease in magnitude. The height at which the radio wave's curvature equals the earth's curvature is defined as the evaporation duct height, which has been found to be a very good parameter to describe the strength of the ducting mechanism [4], [5], [8], [9]. The evaporation duct height can be calculated based on measurements of sea temperature, air temperature, relative humidity, and wind speed using the methods developed by Jeske [4] and Paulus [10]. Using their methods, annual frequency distributions of evaporation duct height have been compiled for many areas of the world based on 15 years of marine surface meteorological observations. These distributions are currently available from the IBM/PC-compatible Engineer's Refractive Effects Prediction System (EREPS) [11].

The propagation model MLAYER used in this paper is the same one used by Hitney and Vieth [5]. It is a numerical waveguide model based on the formalism of Budden [12] developed by Baumgartner and Pappert. This program is briefly described along with some case-study examples in [13]. Results presented here using MLAYER were generated for duct heights in 2-m increments in the identical manner as described in [5], the only difference being the use of propagation factor instead of path loss.

The propagation experiment used in this paper is also the same one used by Hitney and Vieth [5] for the Aegean Sea. The experiment is described in detail by Richter and Hitney [14]. Transmitters and receivers were installed on the Greek Islands of Naxos and Mykonos, respectively, to establish a one-way over-water propagation path of 35 km. Frequencies of 1.0, 3.0, 9.6, 18.0, and 37.4 GHz were used, although in this paper the highest and lowest frequencies are not consid-

Manuscript received November 6, 1989; revised May 1, 1990.

The authors are with the Naval Ocean Systems Center, San Diego, CA 92152-5000.

IEEE Log Number 9037646.

U.S. Government work not protected by U.S. copyright

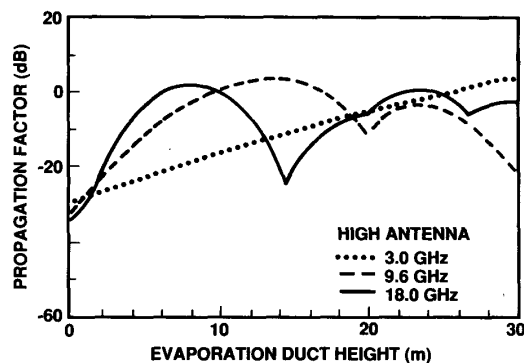


Fig. 1. Propagation factor versus evaporation duct height for the three frequencies studied and the high receiving antenna.

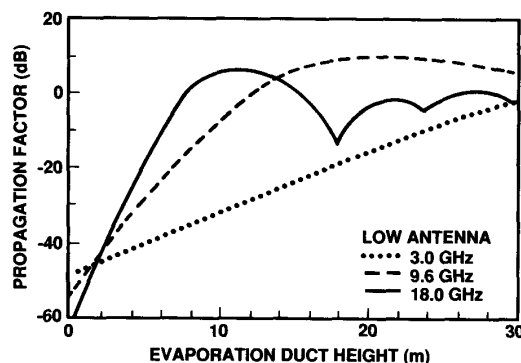


Fig. 2. Propagation factor versus evaporation duct height for the three frequencies studied and the low receiving antenna.

ered. The transmitter heights were 4.8 m above mean sea level (msl) at 3 and 9.6 GHz and 4.5 m above msl at 18 GHz. Three receiver antenna heights were used at most frequencies, although in this paper only the highest and lowest are considered, which will be referred to as high and low. The high antenna was 19.2 m above msl for 3 and 9.6 GHz and 17.8 m above msl for 18 GHz. The low antenna was 4.9 m above msl for 3 and 9.6 GHz and 4.3 m above msl for 18 GHz. Horizontal polarization was used at all frequencies and received signal strength was recorded continuously, switching each 5 min between the three receiving-antenna heights for a complete cycle each 15 minutes. Measurements were made for approximately three weeks each in February, April, August, and November of 1972 at 3 and 9.6 GHz, but only in August and November at 18 GHz. The original data were recorded on paper strip charts using a receiver time constant of 4 s. These data were averaged by eye and entered into a digital data base, from which the results in this paper were prepared.

II. PROPAGATION FACTOR AS A FUNCTION OF DUCT HEIGHT

The M-LAYER model was used for each frequency to generate propagation factors as functions of duct height in 2-m increments for each of the two receiving antennas considered. These results are presented in Fig. 1 for the high antenna and in Fig. 2 for the low antenna for duct heights up to 30 m. In both figures, continuous curves were fit by eye to the discrete 2-m-increment duct-height results to better illustrate the waveguide modal-interference patterns at higher duct heights and frequencies. Some slight errors may therefore have been introduced in these figures, especially at nulls such as the one near 14 m at 18 GHz in Fig. 1.

Note the general behavior in both Figs. 1 and 2 as frequency increases. At 3 GHz, the propagation factor steadily increases with duct height as a result of there being only one important waveguide mode. At 9.6 GHz, there is a more rapid initial increase with duct height than at 3 GHz, but a maximum propagation factor is reached at some duct height. Beyond this duct height, two or more waveguide modes compete to form a complicated propagation factor behavior versus duct height. As frequency increases to 18 GHz, the

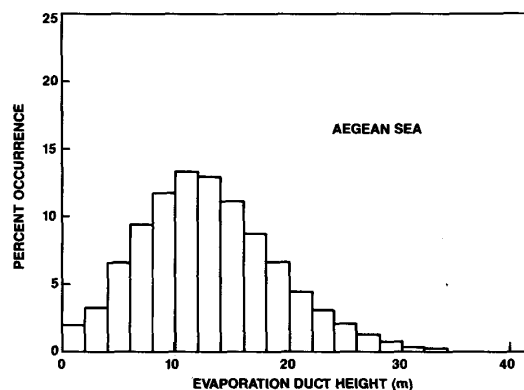


Fig. 3. Histogram of evaporation duct height for the area of the measurements in the Aegean Sea.

initial increase in propagation factor with duct height is yet steeper, with the duct height corresponding to the highest signal occurring at a lower value than at 9.6 GHz. The behavior just described is dependent on receiver (or transmitter) height, especially for the higher frequencies and duct heights, as is evident by an inspection of the differences between Figs. 1 and 2. However, both figures clearly suggest that a frequency-diversity scheme might be employed to substantially improve communication or surveillance capability on such paths, since the best of two signals, such as at 9.6 and 18 GHz, should be much better than either signal alone much of the time.

To quantitatively model the merits of radio-frequency diversity in the evaporation duct, one must have knowledge of the duct-height distribution. Fig. 3 is a histogram of evaporation duct height for that area of the Aegean Sea in which the measurements were taken. Specifically, Fig. 3 derives from the EREPS program [11] for Marsden Square 142, which is the ten-degree latitude by ten-degree longitude square containing the measurement path. The duct-height distribution shown in Fig. 3 is also included numerically in the first column of Table I. Inspection of Fig. 3 or Table I indicates the most common duct heights are in the 10–12 m category, with virtually all duct heights being less than 30 m. Since the 18 GHz data were only collected during the August and

TABLE I
EVAPORATION DUCT HEIGHT FREQUENCY DISTRIBUTIONS FOR THE AEGEAN SEA BASED ON ALL 12 MONTHS, THE AEGEAN SEA FOR AUGUST AND NOVEMBER ONLY, AND FOR MOST OCEAN AREAS OF THE WORLD FOR 12 MONTHS

Duct Height meters	Aegean Sea Annual %	Aegean Sea Aug/Nov %	World Avg Annual %
00 to 02	2.0	1.4	5.4
02 to 04	3.4	1.6	5.0
04 to 06	6.7	4.4	7.2
06 to 08	9.5	6.4	8.2
08 to 10	11.8	8.8	9.2
10 to 12	13.4	11.3	10.4
12 to 14	12.9	12.3	10.9
14 to 16	11.2	12.0	10.5
16 to 18	8.7	10.6	9.2
18 to 20	6.7	8.9	7.5
20 to 22	4.6	6.2	5.8
22 to 24	3.2	5.1	4.1
24 to 26	2.1	3.8	2.7
26 to 28	1.4	2.6	1.7
28 to 30	0.9	1.6	1.0
30 to 32	0.5	1.0	0.5
32 to 34	0.4	0.7	0.3
34 to 36	0.2	0.4	0.2
36 to 38	0.1	0.3	0.1
38 to 40	0.1	0.2	0.0
> 40	0.2	0.4	0.1

November measurement periods, a special distribution covering only these two months is included in Table I. Note the most common duct heights have increased slightly, but the overall distribution is much the same as the annual distribution. Table I also includes a world average annual distribution for comparison, which is similar to both distributions in the Aegean Sea. Combining the distributions in Table I, as appropriate, with the M-LAYER results illustrated in Figs. 1 and 2 then allows either single- or multiple-radio-frequency signal-level distributions to be modeled.

III. SINGLE-FREQUENCY RESULTS

Using the methods outlined in the previous section, cumulative frequency distributions of propagation factor were prepared for each radio frequency separately and compared to measured results from the Greek Islands experiment. Since comparisons were desired between the three frequencies, only the common periods of August and November were considered. Figs. 4-6 show these results for the high antenna at 3, 9.6, and 18 GHz, respectively. These figures show the percent of time the propagation factor exceeds the abscissa value. The solid curves are the modeled or calculated results using M-LAYER and the duct-height distributions from Table I, while the dotted curves are the experimental results. Sample size in each figure refers to the number of 5-min samples in each data set. It should be pointed out these results are nearly the same as those presented by Hitney and Vieth [5], the only differences being the use of propagation factor in lieu of path loss, and the reduced data sets at 3 and 9.6 GHz.

Fig. 4 shows a median (i.e., 50% exceeding) calculated propagation factor at 3 GHz of -9 dB, compared to an observed value of -7 dB. The standard-atmosphere diffraction-field value for this frequency and geometry is -28 dB, which implies calculated and observed median gains over diffraction of 19 and 21 dB, respectively. The disagreement

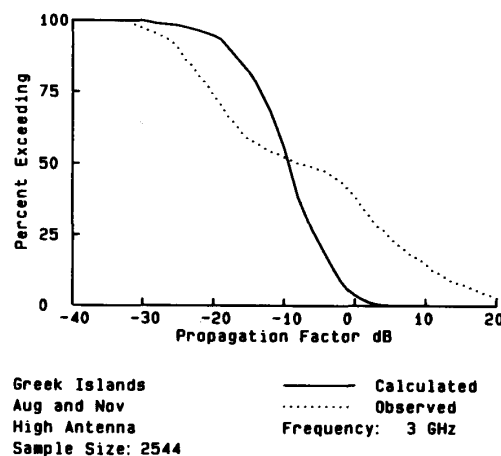


Fig. 4. Calculated and observed cumulative frequency distributions of propagation factor for 3 GHz and the high receiving antenna for August and November.

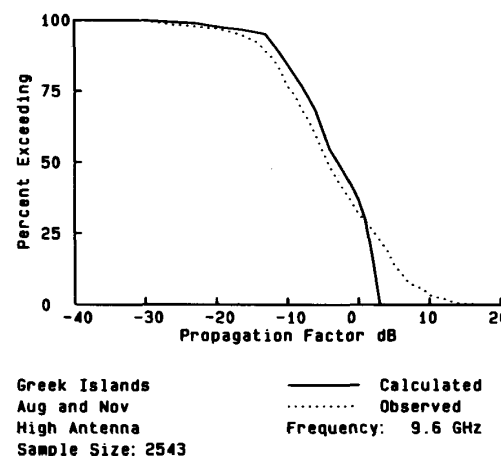


Fig. 5. Calculated and observed cumulative frequency distributions of propagation factor for 9.6 GHz and the high receiving antenna for August and November.

between calculated and observed propagation factors greater than zero at 3 GHz is apparently due to the presence of propagation mechanisms other than the evaporation duct, such as surface-based ducts from elevated trapping layers, as discussed in [5]. In spite of this disagreement, the overall comparison between calculated and observed distributions in Fig. 4 is considered fair, especially when viewed in relation to the diffraction field.

Fig. 5 shows results for 9.6 GHz. Here the calculated and observed median propagation factors are -3 and -4 dB, respectively. Note the overall better agreement of calculated and observed distributions at this frequency than at the lower frequency, which is thought to be a result of the evaporation duct dominating other propagation mechanisms. As with 3 GHz, the greatest discrepancy occurs at the high signal levels. The diffraction-field propagation factor for this geometry and frequency is -31 dB, corresponding to calculated and observed gains of 28 and 27 dB, respectively.

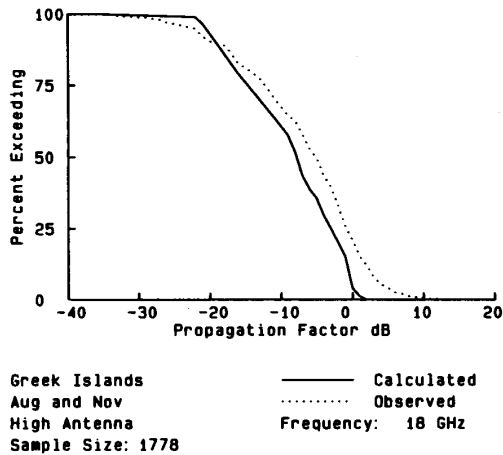


Fig. 6. Calculated and observed cumulative frequency distributions of propagation factor for 18 GHz and the high receiving antenna for August and November.

Fig. 6 illustrates the 18 GHz results. The agreement between the calculated median of -8 dB and the observed median of -5 dB is slightly worse than the 9.6 GHz case, but the overall comparison of the two distributions is quite good. The diffraction-field propagation factor at 18 GHz for this geometry is -35 dB, resulting in a median calculated gain of 27 dB and a median observed gain of 30 dB. Again, the worst disagreement between calculated and observed distributions is for the highest signal levels.

Figs. 4–6 illustrate, as did [5], that the evaporation duct is an important propagation mechanism at the frequencies studied, and can result in substantial gains over diffraction theory. The figures also illustrate that our ability to model distributions of this mechanism's effects is quite good.

IV. MULTIPLE-FREQUENCY EFFECTS

MLAYER results, as illustrated in Figs. 1 and 2, were combined with the evaporation duct-height distributions of Table I to model distributions of the maximum propagation factor of two or three radio frequencies. In other words, distributions were prepared showing the percent of time the highest signal of the two or three frequencies exceeded given values. Observed distributions were prepared from the original Greek Island observation data set by computing propagation factor for each 15-min sample, comparing this factor to the corresponding factor at the other frequency or frequencies, and then selecting the highest propagation factor for that 15-min sample. In some cases, as a result of equipment calibration or failure, data did not exist for all frequencies in question. Only those samples were selected for the observed distributions for which observed data existed at each frequency under consideration. Figs. 7–12 contain a selection of these calculated and observed distributions. Each figure also contains the distributions of the single-frequency propagation factors for reference. These reference distributions are slightly different than those presented in Figs. 4–6 due to the smaller sample size necessary to compute the maximum distributions.

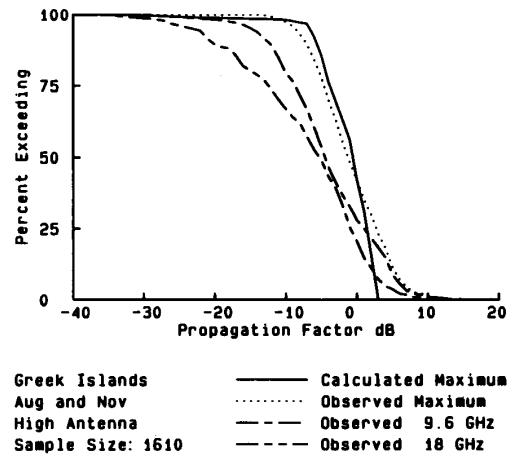


Fig. 7. Calculated and observed cumulative frequency distributions of the greatest propagation factor at 9.6 or 18 GHz for the high antenna during August and November.

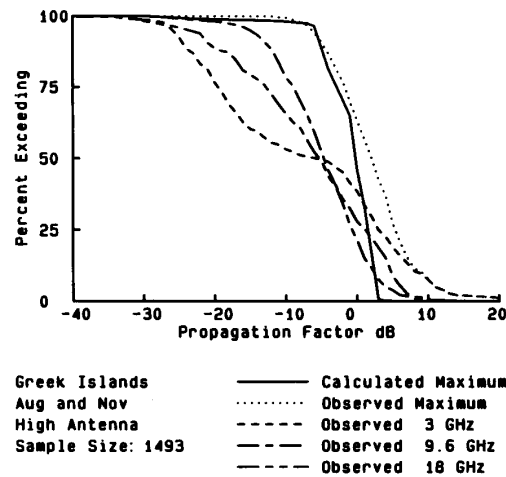


Fig. 8. Calculated and observed cumulative frequency distributions of the greatest propagation factor at 3, 9.6, or 18 GHz for the high antenna during August and November.

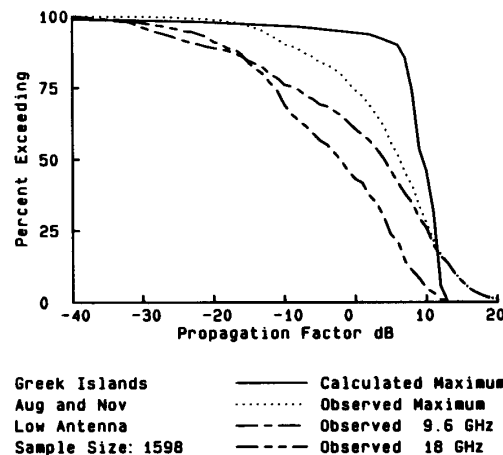


Fig. 9. Calculated and observed cumulative frequency distributions of the greatest propagation factor at 9.6 or 18 GHz for the low antenna during August and November.

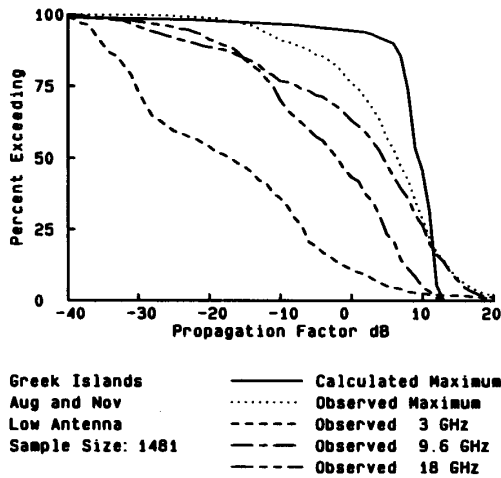


Fig. 10. Calculated and observed cumulative frequency distributions of the greatest propagation factor at 3, 9.6, or 18 GHz for the low antenna during August and November.

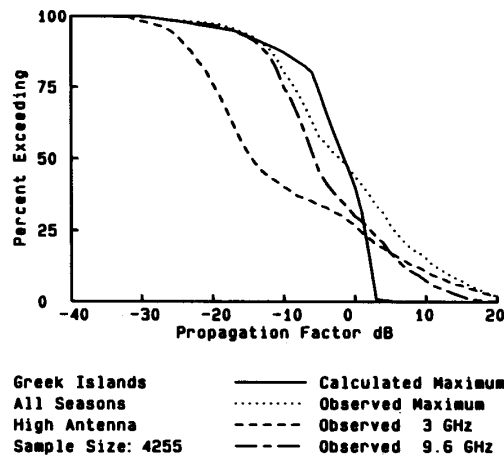


Fig. 11. Calculated and observed cumulative frequency distributions of the greatest propagation factor at 3 or 9.6 GHz for the high antenna during all seasons.

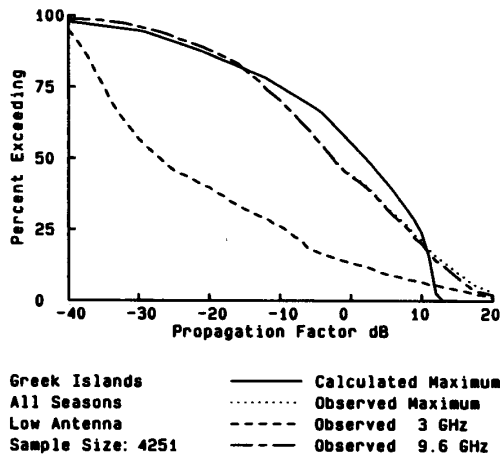


Fig. 12. Calculated and observed cumulative frequency distributions of the greatest propagation factor at 3 or 9.6 GHz for the low antenna during all seasons.

TABLE II
MEDIAN PROPAGATION FACTORS FOR EACH SINGLE FREQUENCY AND FOR THE CALCULATED AND OBSERVED MAXIMUM DISTRIBUTIONS, PLUS THE OBSERVED IMPROVEMENT IN THE MEDIAN OVER THE BEST SINGLE FREQUENCY (H = HIGH ANTENNA; L = LOW ANTENNA; $A + N$ = AUGUST AND NOVEMBER; * = NOT USED)

Fig	Ant	Per	MEDIAN PROPAGATION FACTOR (dB)					
			Frequency (GHz)			Maximums		
			3	9.6	18	Cal	Obs	Imp
7	H	A+N	*	-4	-5	-1	-1	3
8	H	A+N	-6	-5	-5	0	2	7
9	L	A+N	*	4	-2	9	6	2
10	L	A+N	-17	5	-2	9	7	2
11	H	All	-14	-6	*	-1	-2	4
12	L	All	-27	-3	*	2	-3	0

TABLE III
PERCENT OF PROPAGATION FACTOR SAMPLES GREATER THAN -10 dB FOR EACH SINGLE FREQUENCY AND FOR THE CALCULATED AND OBSERVED MAXIMUM DISTRIBUTIONS, PLUS THE OBSERVED IMPROVEMENT IN THE PERCENTAGE OVER THE BEST SINGLE FREQUENCY (H = HIGH ANTENNA; L = LOW ANTENNA; $A + N$ = AUGUST AND NOVEMBER; * = NOT USED)

Fig	Ant	Per	PERCENT GREATER THAN -10 dB					
			Frequency (GHz)			Maximums		
			3	9.6	18	Cal	Obs	Imp
7	H	A+N	*	80	67	98	98	18
8	H	A+N	53	80	67	98	99	19
9	L	A+N	*	77	70	97	91	14
10	L	A+N	36	77	70	97	91	14
11	H	All	40	75	*	87	81	6
12	L	All	26	71	*	75	71	0

Fig. 7 shows the results for the high antenna at 9.6 and 18 GHz. The median single-frequency propagation factor is -4 dB at 9.6 GHz and -5 dB at 18 GHz. Both the calculated and observed maximum distributions show median values of approximately -1 dB, indicating a 3 dB median frequency-diversity enhancement over the best single frequency. Another measure of improvement is the percent of time the maximum signal exceeds a given threshold level. We have arbitrarily chosen a threshold propagation factor of -10 dB for comparisons in this paper. Fig. 7 shows that 67% of the 18 GHz signals exceed this level and 80% of the 9.6 GHz signals exceed the -10 dB level. However the observed maximum of the two signals exceeds -10 dB 98% of the time, for a frequency-diversity improvement of 18% over the best single frequency. The calculated maximum signal is seen to exceed -10 dB 98% of the time also, which is in excellent agreement with the observed value.

The median propagation factors and their observed improvements due to frequency diversity are summarized in Table III for all the cases presented in Figs. 7-12. Likewise, the percent of propagation factors exceeding -10 dB, and the observed frequency-diversity improvement in this percentage, are summarized in Table III for Figs. 7-12. The improvement in the median levels varied from 0-7 dB, while the improvement in percentage greater than -10 dB varied from 0-19. Least affected were the cases that paired 3 and 9.6 GHz, especially for the low antenna. This behavior is consistent with the theoretical results presented in Figs. 1 and 2, which show an improvement for the high antenna would be expected only for those rare duct heights in excess of about 20 m, and an improvement for the low antenna would virtually never occur.

V. DISCUSSION

The comparisons presented here indicate that statistical modeling of evaporation duct effects, either considering one frequency at a time or the best of multiple frequencies, is in good agreement with observations. It must be pointed out, however, that some height-diversity effects are included in both the modeled and observed results when 9.6 and 18 GHz are compared. The height difference of the transmitter antennas, from 4.8 to 4.5 m above msl, and the differences of the receiver antennas from 19.2 to 17.8 m above msl at the high position and 4.9 to 4.3 m above msl at the low position, were not thought to be significant. To check this hypothesis, the 18 GHz modeled results were recalculated using the same geometry as the 3 and 9.6 GHz cases. Except near the modal interference nulls, the differences in propagation factor resulting from these slight height differences were generally less than 3 dB, which is far less than the differences in propagation factor between 9.6 and 18 GHz. Thus the slight height-diversity effects mentioned above should have a minimal impact on the frequency-diversity results presented here.

The frequency-diversity advantage combining 9.6 and 18 GHz is clear from the appropriate figures and Tables II and III. The additional advantage offered by combining the third frequency of 3 GHz is not so clear. Although Table II shows the observed median improvement to go from 3 to 7 dB for Figs. 7 and 8, the corresponding improvement in the percentage of propagation factors greater than -10 dB only goes from 18 to 19. However, these improvements are at the 98 and 99% levels. Had a different threshold been chosen, such as 0 dB, then the improvements would have been observed to go from 14 to 26 dB, for 9.6 and 18 GHz and for all three frequencies, respectively. Thus the three-frequency improvement can be significantly better than the two-frequency improvement. For the low antenna, as evidenced by Figs. 9 and 10, there was almost no additional improvement by combining the three frequencies. This behavior is expected based on Fig. 2, which shows 9.6 GHz almost always outperforms 3 GHz.

The implications of the results presented here to communication or surveillance systems could be substantial. The selection of a propagation-factor threshold at -10 dB was completely arbitrary, and actual thresholds for any proposed real system would have to be carefully calculated and considered. These performance thresholds would be dependent in general on the frequencies chosen, thus making a reference to -10 dB at both 9.6 and 18 GHz, for example, unrealistic. However, the prospect of improving a channel's long-term performance level from 80 to 98% is very significant, and seems to justify the calculations required to assess its practicality in real-world applications.

There may be a natural preference of frequencies that maximize performance in the evaporation duct that is largely independent of geometry or location. Although each application should be considered independently, Table I illustrates that typical evaporation duct height distributions concentrate most duct heights in the 0–20 m range. The interference nulls in Figs. 1 and 2 can be explained in terms of waveguide theory as multiple waveguide modes of low attenuation rate

interfering with each other. Below 20-m duct heights, one such mode dominates at 9.6 GHz. At 18 GHz, one mode dominates up to about 10 m duct heights, and two modes interfere between 10 and 20 m duct heights. The exact modal-interference patterns are dependent on transmitter and receiver heights, as illustrated by the differences between Figs. 1 and 2. However, the general behavior is the same. At low duct heights, 18 GHz is clearly better because of the rapid increase of propagation factor with increasing duct height. Beyond 10-m duct heights, the two competing modes at 18 GHz begin to interfere, but in this range the 9.6 GHz signal will be quite strong due to the dominance of its single mode. In designing an optimum frequency-diversity scheme, it appears that one frequency near 10 GHz and the other between 15 and 20 GHz would be best. It would be inadvisable, however, to select a second frequency that is an exact multiple of the first, since then at some duct height their modal-interference nulls are likely to coincide. Also, it is probably not desirable to select a frequency above 20 GHz, since gaseous absorption, particularly from water vapor, will start to counteract the beneficial effects of the evaporation duct. Also it is believed [13], [14] that sea-surface roughness effects will decrease the gain of the evaporation-duct at frequencies above 20 GHz. For radar applications, a good selection would appear to be one frequency in *X*-band and one in *Ku*-band. It is interesting to note in retrospect that the selection of the 9.6 and 18 GHz frequencies in the Greek Islands experiment perfectly matched the above arguments.

VI. CONCLUSION

Both theoretical and experimental results indicate that frequency diversity can be used to maximize benefits from the evaporation duct on over-the-horizon, over-water paths. Although each proposed application should be individually examined, one frequency near 10 GHz and a second between 15 and 20 GHz should give substantial improvements over a single-frequency system.

ACKNOWLEDGMENT

The authors wish to thank the Office of Naval Technology, Code 22, for their continuing support of tropospheric radio propagation modeling programs, and Mr. Claude Hattan of the Naval Ocean Systems Center for providing the MLAYER calculations used in this study.

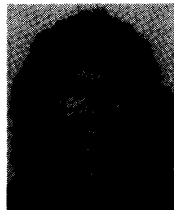
REFERENCES

- [1] C. L. Pekeris, "Wave theoretical interpretation of propagation of 10-centimeter and 3-centimeter waves in low ocean ducts," *Proc. IRE*, vol. 35, pp. 453–462, May 1947.
- [2] M. Katzin, R. W. Bauchman, and W. Binnian, "3- and 9-centimeter propagation in low ocean ducts," *Proc. IRE*, vol. 35, pp. 891–905, Sept. 1947.
- [3] H. Jeske and K. Brocks, "Comparison of experiments on duct propagation above the sea with the mode theory of Booker and Walkinshaw," *Radio Sci.*, vol. 1, no. 8, pp. 891–895, Aug. 1966.
- [4] H. Jeske, "State and limits of prediction methods of radar wave propagation conditions over the sea," in *Modern Topics in Microwave Propagation and Air-Sea Interaction*, A. Zanca, Ed. New York: Reidel, 1973, pp. 131–148.
- [5] H. V. Hitney and R. Vieth, "Statistical assessment of evaporation duct propagation," *IEEE Trans. Antennas Propagat.*, vol. 38, pp. 794–799, June 1990.

- [6] IEEE Standard 211-1977.
- [7] D. E. Kerr, "Fundamental concepts," in *Propagation of Short Radio Waves*, D. E. Kerr, Ed. New York: McGraw-Hill, 1951, pp. 27-41.
- [8] S. Rotheram, "Radiowave propagation in the evaporation duct," *Marconi Rev.*, vol. XXXVII, pp. 18-40, 1974.
- [9] W. L. Patterson, "Comparison of evaporation duct and path loss models," *Radio Sci.*, vol. 20, no. 5, pp. 1061-1068, Sept.-Oct. 1985.
- [10] R. A. Paulus, "Practical application of an evaporation duct model," *Radio Sci.*, vol. 20, no. 4, pp. 887-896, July-Aug. 1985.
- [11] W. L. Patterson *et al.*, "Engineer's refractive effects prediction system (EREPS) revision 2.0," Naval Ocean Syst. Cent., Tech. Doc. 1342 Rev. 2.0, Feb. 1990.
- [12] K. G. Budden, *The Wave-Guide Mode Theory of Wave Propagation*. London, England: Logos, 1961.
- [13] H. V. Hitney, J. H. Richter, R. A. Pappert, K. D. Anderson, and G. B. Baumgartner, "Tropospheric radio wave propagation," *Proc. IEEE*, vol. 73, no. 2, Feb. 1985.
- [14] J. H. Richter and H. V. Hitney, "Antenna heights for the optimum

utilization of the evaporation duct," vols. 1 and 2, Naval Ocean Syst. Cent., Tech. Doc. 1209, Jan. 1988.

Herbert V. Hitney, for a photograph and biography please see page 799 of the June 1990 issue of this TRANSACTIONS.



Linda R. Hitney received the B.A. degree in mathematics and the B.S. degree in computer science from San Diego State University, San Diego, CA, in 1969 and 1985, respectively.

She has worked in the Ionospheric Branch of the Ocean and Atmospheric Sciences Division of the Naval Ocean Systems Center since 1969 on a variety of wave-propagation projects.